Int. J. Multiphase Flow, Vol. 3, pp. 459–469. Pergamon/Elsevier, 1977. Printed in Great Britain

THE RESIDENCE TIME DISTRIBUTION OF SOLID AND LIQUID IN MULTISTAGE BUBBLE COLUMNS IN THE COCURRENT FLOW OF GAS, LIQUID AND SUSPENDED SOLID†

E. BLASS
Institut für Verfahrenstechnik der Technischen Universität München, West Germany

and

W. CORNELIUS
Preussag, Huttenwerk Harz, Goslar, West Germany

(*Received* 4 *April* 1976)

Abstract—Multiphase flow in a multistage bubble column reaction is investigated experimentally. Within the range of parameters studied, it is possible to neglect the influence of plate geometry and liquid throughput on the liquid hold-up. Additionally, the distance between plates and solid concentration had negligible effect on the liquid hold-up.

The reaction chamber of a multistage bubble column reactor is divided by equally spaced orifice plates into a corresponding number of segments. Gas, liquid and/or solid particles suspended in the liquid phase are pumped upwards cocurrently through the equipment. The orifice plates hinder or reduce the axial mixing of the reactor volume incrementally according to working conditions, and improve the residence time distribution of liquid and solid. The gain, relative to time and volume, of chemical reactions occurring is also increased.

In earlier papers, Blass, Koch & Cornelius (1972, 1973), reported mainly about the flow patterns and results of flow investigations in the case of cocurrent flow of gas and liquid. The present paper relates to these investigations and summarizes additional results with cocurrent flow of gas, liquid and solid suspensions. The experimental investigations were performed varying geometric, operative and material parameters.

Experimental size and pilot plant

Table 1 contains the range of variation of geometric and operative parameters as well as the combinations of materials used for various runs. The aperture ratio of the perforated plates, the cross sectional area of holes relative to column cross section, was varied within the wide range between 1.1 and 36%.

The brass perforated plates were sealed against the wall of the column with moss rubber. The sharp-edged holes were produced with a tolerance of $\pm 50\ \mu m$. The superficial gas velocity was varied within the specified range, which is considerable for the technical use of bubble columns. The superficial liquid velocity was relatively slow to obtain adequately long residence times. Sand was as the solid phase only in very low concentrations, because obtaining a large amount with a narrow spectrum of particle diameter was extremely time consuming. For realization of higher concentrations of solid, pre-sorted glass spheres were bought.

The experimental apparatus is shown in figure 1. The principal item is the acrylic glass reactor, 3250 mm in height and 140 mm inner diameter, permitting the flow to be observed and filmed by a high speed camera.

The gas phase was oil free compressed air, dried before flowmeter measurement and

†From a lecture at the annual meeting of the Verfahrensingenieure, 30 September–2 Oktober 1975 in Karlsruhe.

Table 1. Experimental parameter ranges

Inner diameter of the reactor	140 mm
Reactor height	3250 mm
Plate distance	534 and 700 mm
Hole diameter	2 and 4 mm
Free cross section of the holes of a perforated plate, relative to column cross section, φ	0.011–0.36
Systems:	
Water–air	
Water–air–sand	
Water–air–glass-spheres	
Mass density of sand	2.63 g/cm³
Mass density of glass spheres	2.45 g/cm³
Mean diameter of the sandcorns	60 μm, 78 μm, 200 μm
Mean diameter of the glass spheres	48 μm, 78 μm, 800 μm
Volume flow of gas (1 bar, 20°C)	0.9–25 m³/h
Mean superficial gas velocity	0.015–0.45 m/s
Volume flow of liquid	30–550 l./h
Superficial velocity of liquid	5×10^{-4}–1×10^{-2} m/s

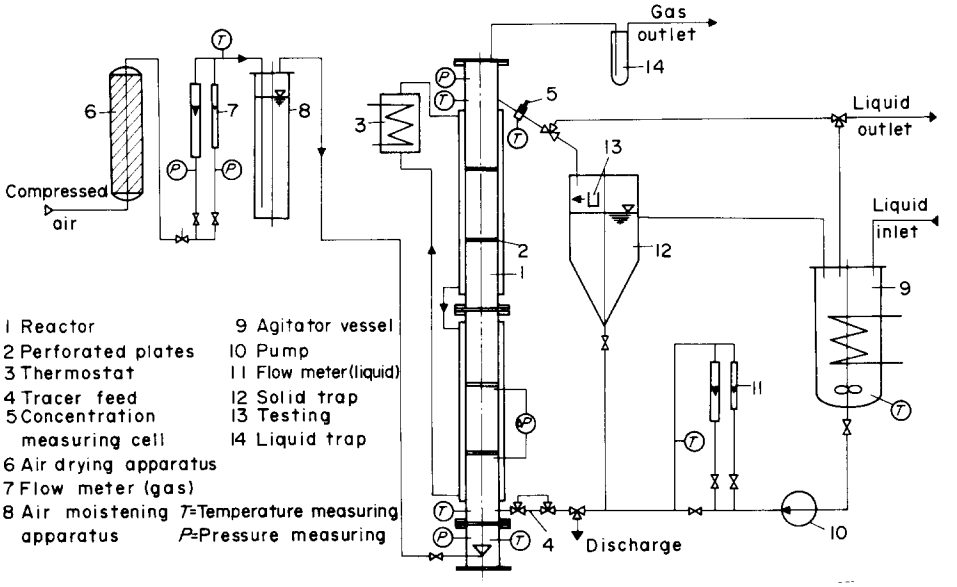

Figure 1. Schematic of experimental plant.

subsequently saturated with water vapor. The liquid phase was water, which could be directed in continuous running as well as in circular running with temperature control in a stirrer vessel. The lowest perforated plate was used as a gas distributor and only gas flowed through it the liquid and suspended solid entering immediately above that perforated plate. Liquid and suspension exited the upper section of the reactor such that the same liquid holdup always existed above the highest perforated plate as in any central section. Return flow from the outlet into the highest cell was impossible. Thus the lowest and the highest section of the reactor should have a behavior somewhat different from that of the central sections. This will be discussed in connection with the measurements of residence time.

In *continuous running*, the residence time distribution of water was measured up to solid concentrations of nearly 3.5%. Gas, liquid and solid were conducted in cocurrent flow. The residence time distribution of solid was considered only with very low solid concentrations. The differential distribution function of water was obtained from the measurement of conductivity at the exit of the reactor in response to a pulsed input (δ-input) of aqueous solution of sodium chloride at the entry of the reactor. For measuring the residence time of solid, 10–30 g sand with a radioactive tracer of scandium 46 (Schulze–Pillot 1970) was placed in the by-pass

line in position 4. Upon reversal of the ball valves, the radioactive sand was washed into the apparatus as an impulse. The time slope of γ-ray intensity was measured as a response function at the exit of the reactor with a scintillation meter (5). The measured intensity of radiation can be calibrated to the number of particles in the measuring volume only, if the number and the activity of the marked particles are sufficiently high.

In *circular running*, higher volume concentrations of solid up to nearly 3.5% were used. The circuit design of the plant should prevent any throughput of solid through the circulating pump 10, in order to preserve the original grain-size spectrum. To this end, solid and liquid were separated in the trap 12 coupled at the outlet side of the reactor. The main part of liquid passed through the temperature controlled stirrer vessel 9, and was reintroduced into the reactor by the circulating pump 10 (speed-regulated Mohno-pump, free of pulsations). The glass spheres, settled out in the trap 12, were carried out of the trap cone by a small bypass flow of liquid and remixed with the main liquid flow. By varying the liquid level in the trap 12, i.e. the excess hydrostatic pressure against the bubble bed in the reactor, the partial liquid flow could be regulated, so that no solid accumulated in the trap. This assured that the transport concentration of solid did not vary during many hours of testing. The transport concentration could be adjusted by the relation of main and bypass liquid flow. If it can now be established that the residence time distribution of liquid is not essentially affected by the suspended solid, and that no solid is deposited in the apparatus, then it is sufficient to know the residence time distribution of liquid and the ratio of transport and volume concentration c_T/c_R of solid for the determination of the residence time distribution of solid. Proof of this is furnished below. Certainly, the procedure is not extensible to unlimited solid concentrations, but causes essentially less display than measuring the residence time of solid by radioactive marking.

For the determination of the volume concentration of solid c_R, (equation [7]), the volumes of liquid and solid in the reactor must be measured. For the analysis of the transport concentration c_T, (equation [8]), the volume flows of both phases must be measured. The volume of solid could be determined by simultaneously quickly turning off the gas input and the inlet and outlet of suspension flow, followed by flushing out, filtering and drying. The volume flows of solid and liquid were measured by the receiver 13 in the free inlet of suspension into the trap 12, Cornelius (1975).

RESIDENCE TIME DISTRIBUTION OF LIQUID

Obviously, the multistage bubble column can be compared with a multistage agitator vessel concerning the residence time distribution of liquid. Thus the results of measurement can be compared with the residence time behavior calculated by the tanks in a series model. The dimensionless differential distribution function E_L is defined as follows:

$$E_L(t) \equiv -\frac{1}{\mathring{M}_L}\frac{\mathrm{d}\mathring{M}_L}{\mathrm{d}t}, \qquad [1]$$

where $\mathring{M}_L$ is the mass flow rate of liquid and t is time. For a series connection of N equal, homogeneously mixed stages without inner and outer backflow with stationary throughput (the so-called mixing stage cascade), this function arises in the following form, Kardos (1969):

$$E(\theta_L) = \frac{N^N}{(N-1)!}\,\theta_L{}^{N-1}\,\mathrm{e}^{-N\theta_L}, \qquad [2]$$

where $\theta_L = t/\bar{t}_r$; $\bar{t}_r$ is the mean residence time.

But the multistage bubble column can also run with inner backflow by corresponding operating conditions, if liquid drops back through the orifices of the perforated plates. Equation (2) is also valid for this operating condition, as far as the stages are homogeneously mixed.

However, the factor N is no longer in conformity with the number of real stages, but only an accommodating parameter, which is designated as a number of effective stages. This number is always smaller than the number of real stages and can be evaluated by comparison of the measured distribution function and the function calculated in [2].

Figure 2 shows a characteristic choice of measured residence time distributions of liquid.

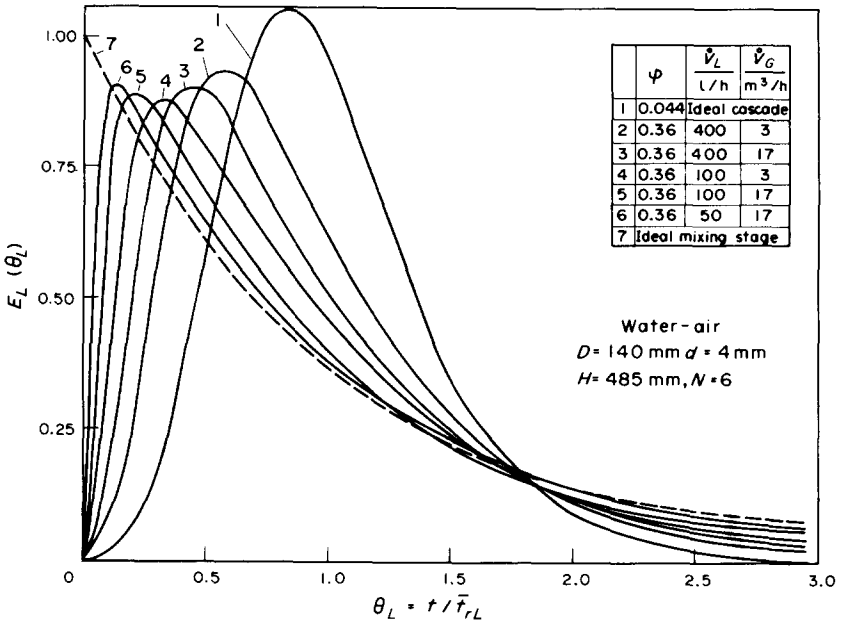

	φ	$\dot{V}_L$ l/h	$\dot{V}_G$ m³/h
1	0.044	Ideal cascade	
2	0.36	400	3
3	0.36	400	17
4	0.36	100	3
5	0.36	100	17
6	0.36	50	17
7	Ideal mixing stage		

Figure 2. Residence time distribution of liquid E_L.

Measuring curve 1 coincides with the residence time characteristics of a series of ideal mixing stages. No influence of gas and liquid flow rate upon residence time characteristics can be observed by using the low aperture ratio, 0.044, of the perforated plates. But by using the highest aperture ratio, 0.36, the residence time distribution approaches the curve of a single fully mixed stirred vessel (curve 7) with increased gas flow rate and decreased liquid flow rate. The residence time distributions become broader in undesired way. To explain these tendencies, the back mixing by dropping back of liquid from stage to stage, but not an insufficient mixing within the single stage, can be cited.

The lowest liquid flow rates caused an immediate distribution of color injection among the whole content of a single stage, whereas clear color gradations were perceptible from stage to stage. A backflow of liquid to the underlaying stage can be most clearly illustrated for this case, in which a gas cushion has arisen below the perforated plates. This operating case is schematically shown in figure 3. The gas cushions below the perforated plates increase with increasing gas flow rate. Thus the oscillations of the bubble bed have to grow in order to reach the next perforated plate and thereby to effect the axial liquid transport. These oscillations cause local and temporary fluctuations of pressure, which are intensified by the likewise enhanced nonsteady whirling flow in the bubble bed. Additionally, the liquid holdup decreases with increasing gas cushion and thus also increase the necessary gas pressure within the gas cushions. If this results in the pressure above the perforated plate to be higher than below it, backmixing sets in. This tendency is reversed in case of very high gas flow rates. Then the upward momentum of gas prevents the liquid backflow through the orifices. For this case there are no systematic results, since the gas flow rate could not be increased without restriction. The liquid holdup in the stages increases with increasing liquid flow rate. Simultaneously, the fluctuations of pressure decrease as a consequence of the reduced oscillations of the bubble bed. This implies the diminution of backmixing with increasing liquid flow rate.

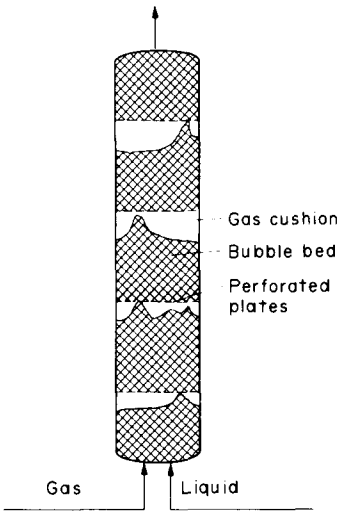

Figure 3. Multistage bubble column with gas-cushion operation.

The number of effective stages was evaluated with the aid of the statistical central moments, which are computable by the residence time distributions. The numbers of effective stages, evaluated from the second, third and fourth central moment, differed from each other only within the accuracy of evaluation. Thus it has been demonstrated that multistage bubble columns with inner back flow obey the laws of ideal mixing stage model and do not exhibit any region of dead flow, Richards & Spörri (1972). The empirical correlation of the number of effective stages succeeded as is shown in figure 4. The compensating curve obeys the following equation:

$$\frac{N_{\text{eff}}}{N} = 1.061 \left(\frac{\text{m}}{\text{s}}\right)^{-0.19} \left(\frac{\bar{w}_{GD}\,\varphi}{w_{Ld}^2}\right)^{-0.19} \qquad [3]$$

where $\bar{w}_{GD}$ is the mean superficial velocity of gas, w_{Ld} is the orifice liquid velocity of the plates, and φ is the cross sectional area of holes, relative to column cross section. Limits of validity are as follows:

$$1.3\frac{\text{s}}{\text{m}} < \frac{\bar{w}_{GD}\,\varphi}{w_{Ld}^2} \leqq 10^3 \frac{\text{s}}{\text{m}},$$

$$0.044 < \varphi \leqq 0.36.$$

Below an abscissa value of 1.3 s/m and for $\varphi \leqq 0.044$, the multistage bubble column shows the same behavior as an ideal mixing stage cascade, so that $N_{\text{eff}}/N = 1$. Unfortunately, there are only experimental results for the water–air system. Therefore it is not yet possible at present, to confirm a dimensionless abscissa term by experimental results. This term might contain the densities and viscosities of both phases and the surface tension. The mean quadratic error is $\pm 4.8\%$. In [3], $\bar{w}_{GD}$ is the mean superficial gas velocity, i.e. the ratio of mean volumetric gas flow rate and cross sectional column area. The mean volumetric gas flow rate was measured with a rotameter and converted to the mean arithmetic value of inlet and outlet pressure on the reactor by the equation of state of ideal gases. The real superficial gas velocity on reactor inlet and outlet—dependent on gas and liquid flow rate—is 9–11% lower or higher than the used mean value. The choice of the reference gas velocity does not significantly affect the result of [3] due to the small exponent, 0.19.

As a result of the design of the apparatus, the end sections of the reactor are anomalous in their behavior as registered by the measurement of residence time. There is no liquid

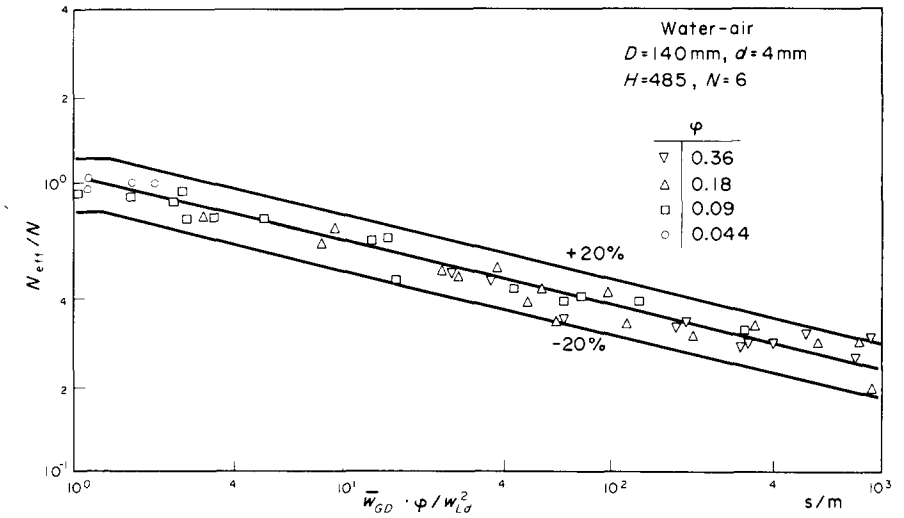

Figure 4. Related number of effective stages (N_{eff}/N) as a function of liquid and gas velocity (w_{Ld}, $\bar{w}_{GD}$) respectively of the aperture ratio of perforated plates (φ).

backmixing out of the lowest and into the highest section. The error caused by the end sections is reduced with increasing number of stages and decreasing backflow. From investigations of Kats & Genin (1966) in bubble columns with 5 and 10 sections, the error due to the end sections is negligible within the range of these stage numbers even in cases of considerable backmixing.

Technically interesting stage numbers are greater than 5 in any case.

Figure 5 shows the size of backflows $\dot{R}_L$ through the perforated plates during backmixing. These backflows are calculated from the statistical moments of residence time distribution with

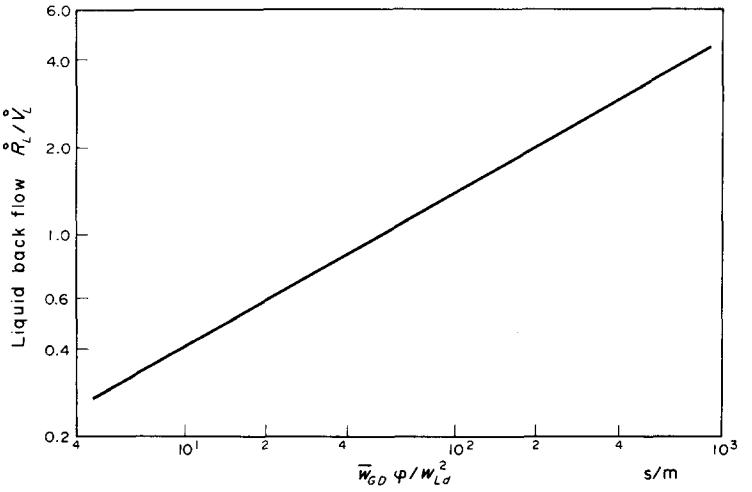

Figure 5. Related liquid back flow ($\dot{R}_L/\dot{V}_L$) as a function of liquid and gas velocity (w_{Ld}, w_{GD}) with respect to the aperature ratio of perforated plates (φ).

the aid of numerical solutions of the differential equations for the cell model enlarged by back flows, Kats & Genin (1966) and Haddad & Wolf (1967). After that the backflow in case of most unfavourable experimental conditions can reach the fivefold value of liquid flow rate. The backmixing deteriorates the chemical exchange, as well as the exploitation of energy for the phase transport through the reactor.

Within the variations of parameters undertaken in the present work, the content of solid does not strongly influence the residence time of liquid.

RESIDENCE TIME DISTRIBUTION OF SOLID

If the solid phase is distributed sufficiently uniformly in the reactor the residence time behavior must be describable by the mixing cell model:

$$E_S(\theta_S) = \frac{N^N}{(N-1)!}\,\theta_S^{N-1}\,e^{-N\theta_S}, \qquad [4]$$

when

$$\theta_S = t/\bar{t}_{rS}. \qquad [5]$$

The proportion of the mean residence time of solid and of liquid can be expressed by the volume concentration c_R and the transport concentration c_T,

$$\frac{\bar{t}_{rS}}{\bar{t}_{rL}} = \frac{c_R}{c_T}\frac{1-c_T}{1-c_R}, \qquad [6]$$

in which

$$c_R = V_S/(V_S + V_L), \qquad [7]$$

and

$$c_T = \mathring{V}_S/(\mathring{V}_S + \mathring{V}_L). \qquad [8]$$

For small values of c_R and c_T [6] can be transformed to

$$\bar{t}_{rS} = \bar{t}_{rL}c_R/c_T. \qquad [9]$$

If in [5] the mean residence time of solid $\bar{t}_{rS}$ is replaced by [9], it follows from [4] for the residence time distribution of solid:

$$E_S(\theta_L) = \frac{N^N}{(N-1)!}\left[\frac{c_T}{c_R}\theta_L\right]^{N-1} e^{-[N(c_T/c_R)\theta_L]}. \qquad [10]$$

Because the residence time distribution of liquid is not strongly influenced by the solid within the range of relatively small solid concentrations, the residence time distribution of solid can be calculated be extending the measured residence time distribution of liquid, according to [10], with the measured proportion c_T/c_R.

The residence time measurement with the aid of radioactive traced sand allows the examination of this idea. Figure 6 shows the results. On the ordinate the number of the marked particles c'_s in the measuring volume related to the total number of marked particles $c'_{s\max}$ is calculated and is not, as in figure 2, related to the total quantity, because the experiments could not be followed to the total solid discharge. The abscissa shows the residence time t_{rL}. The results are shown for the named group of parameters. The theoretical residence time distribution of solid by slipless transport, which is identical with the residence time distribution of liquid, is drawn as a dotted line.

The symbols shown represent the experimental results. After that the solid stays much longer in the reactor than the liquid, and the longer the solid stays in the reactor, the smaller is the superficial velocity. As the tails of the residence time curves could not be measured by the radioactive tracer method, the residence time curves were not drawn with the aid of the

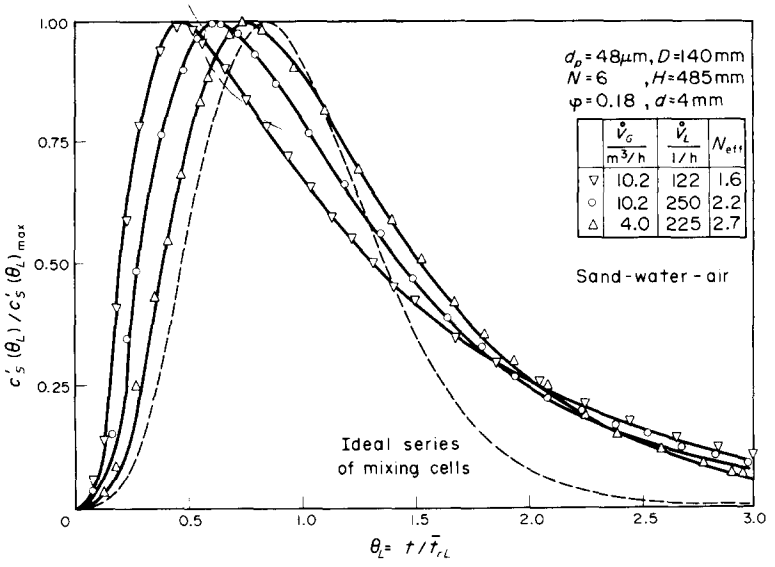

	$\dot{V}_G$ m³/h	$\dot{V}_L$ l/h	N_{eff}
▽	10.2	122	1.6
○	10.2	250	2.2
△	4.0	225	2.7

Figure 6. Reduced residence time distribution of the solid ($c'_S/c'_{S\,max}$) with backmixing.

statistical moments as in case of two-phase flow. On the contrary, the abscissa value of the maximum of the theoretical distribution ($c_T/c_R = 1$) was divided by the abscissa value of the maximum of the measured distribution, from which, assuming validity of the cell model, the proportion of transport and volume concentration follow directly:

$$\frac{\bar{t}_{rL}}{\bar{t}_{rS}} = \frac{c_T}{c_R}. \qquad [11]$$

With this concentration proportion the curves were calculated by the cell model. The agreement between the experimental results and the calculated curves shows that the residence time distribution of solid is describable with sufficient exactness by the cell model in this range of experiments. Some differences are explicable from the fact that the measured distributions are envelope curves of the residence time distribution of the single corn fractions of the feed.

In this manner the capacity of the ideas explained by [4]–[11] could have been proved by the residence time distribution with radioactive sand. Therefore the experiments with higher solid concentration were restricted to residence time distribution of liquid and to the measurement of the proportion c_T/c_R. It appeared that the proportion amounts by increase of superficial gas velocity $\bar{w}_{GD}$ and increase of the liquid velocity are related to the cross sectional area of the holes of the perforated plate w_{Ld}. The greater the diameter of the particles and the free hole cross section, the smaller becomes the proportion c_T/c_R because of the increasing tendency of sedimentation and the growing of the backmixing from cell to cell. With small throughput of gas and large particle diameter the dispersed energy does not suffice for a time to prevent the deposition of some particles on the perforated plates. A steady deposition of particles could not be observed in the whole range of experimental parameters down to superficial gas velocities of only 5 cm/s and particle diameter of 250 μm. This corresponds to the results of single stage, three phase fluidised bed, Imafuku *et al.* (1968).

Characteristic dimensionless groups for three phase suspending processes are the Froude number of gas Fr_{GS} and liquid Fr_{LS}, Mach (1968). The results could also be represented successfully in a manner as shown in figure 7. The experimental data of residence time measurements with radioactive traced sand are fitted well in this graph. The empirical equations of the compensating curves are:

$$\frac{c_T}{c_R} = 0.065 Fr_{LS}^{0.077} Fr_{GS}^{0.2} \left(\frac{d}{d_p}\right)^{0.39} \qquad [12]$$

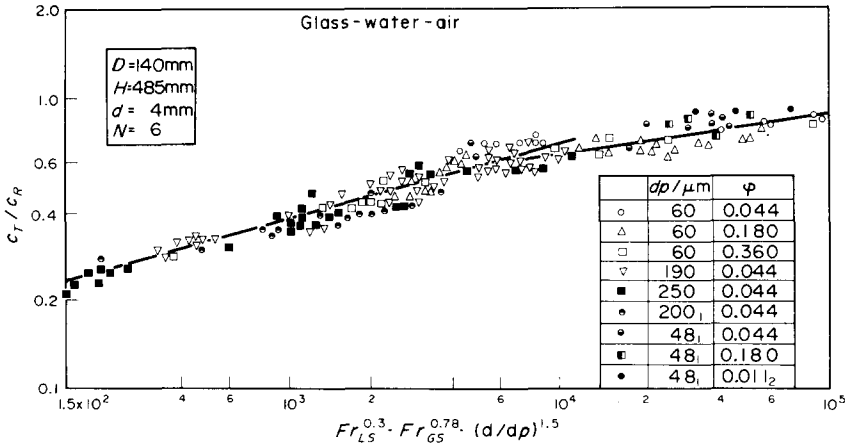

Figure 7. Relation of transport and volume concentration (c_T/c_R) of solid as a function of the Froude numbers of gas (Fr_{GS}) and liquid (Fr_{LS}). (1) c_T/c_R calculated from residence time distributions of sand, (2) $d = 2$ mm.

within the range

$$1.5 \cdot 10^2 \leq Fr_{LS}^{0.3} Fr_{GS}^{0.78} \left(\frac{d}{d_p}\right)^{1.5} \leq 10^4$$

respectively

$$\frac{c_T}{c_R} = 0.17 Fr_{LS}^{0.043} Fr_{GS}^{0.112} \left(\frac{d}{d_p}\right)^{0.216} \qquad [13]$$

within the range

$$10^4 \leq Fr_{LS}^{0.3} \cdot Fr_{GS}^{0.78} \left(\frac{d}{d_p}\right)^{1.5} \leq 10^5.$$

The Froude numbers Fr_{LS} and Fr_{GS} are formed as follows:

$$Fr_{LS} = \frac{w_{LD}^2}{g d_p}; \quad Fr_{GS} = \frac{\bar{w}_{GD}^2}{g d_p};$$

where g is the acceleration due to gravity. The mean quadratic deviation amount to ±5.4%. The concentration of solid volume does not influence the quotient c_T/c_R as shown with a regression analysis, e.g. the interaction between the particles does not influence the flow characteristics of the particles within the range of these experimental parameters.

LIQUID HOLD-UP

The liquid hold-up related to the reactor volume, ϵ_L, was reported by Blass & Cornelius (1973). ϵ_L has been measured in the center section of reactor after rapid and simultaneous stop of the gas and liquid feed. The measured values correspond to the mean liquid hold-up in the reactor computed with the first statistical moment of the residence distribution within the range of the accuracy. Accordingly the relative liquid hold-up becomes perceptibly smaller with growing gas throughput and increases only little with growing liquid throughput. This behaviour can be explained in the same way as the tendencies of backflow. Beyond the findings given by Blass & Cornelius (1973) this work gives the following results.

It is possible to neglect the influence of the plate geometry and the liquid throughput on the relative fluid hold-up within the limits of the experiments. Also, the distance separating the perforated plates causes no measurable differences in the results in the range between 400 and 700 mm and the solid suspended in liquid negligibly influences the relative liquid hold-up within the range of the investigated concentrations.

Differing from this Molzahn (1971) reported that in a single stage bubble column the solid suspension leads to an increase of the relative liquid hold-up, caused by an increase of the inclination of coalescence due to the presence of suspended solid. The larger bubble diameters lead to an increased bubble rise velocity, shorter bubble residence time into the bubble bed, and an increase of the relative liquid hold-up. In bubble column cascades this influence does not become significant because the gas bubbles were regularly resized by the perforated plates and thus relatively small cell hights correspond to only small bubbles.

The experimental results follow [14] and [15]: Within the range

$$0 \leq Fr_{GD} \leq 1.8 \cdot 10^{-3},$$
$$\epsilon_L = 1 - 0.1 \left(Fr_{GD} \frac{\rho_G}{\rho_L - \rho_G} \right)^{0.5}, \qquad [14]$$

within the range

$$1.8 \cdot 10^{-3} < Fr_{GD} < 220 \cdot 10^{-3},$$
$$\epsilon_L = 0.16 \left(Fr_{GD} \frac{\rho_G}{\rho_L - \rho_G} \right)^{-0.14}. \qquad [15]$$

In [14] and [15], Fr_{GD} can be determined with local superficial gas velocity w_{GD}, if the liquid hold-up of one cell is to be determined, or with the mean velocity $\bar{w}_{GD}$, if the mean liquid hold-up of the reactor is to be calculated.

The same is valid for the gas density ρ_G. The Froude number Fr_{GD} is defined as follows

$$Fr_{GD} = \frac{w_{GD}^2}{g \cdot D}.$$

The mean quadratic deviation between the measured points and the compensating function amounts to $\pm 2.0\%$. Both equations are determined only with the water–air system. The influence of the densities and the column diameter expressed by these equations could not be established by experiments. But the influence of such dimensionless groups on the liquid hold-up were confirmed several times in single stage bubble columns.

The gas pressure drop of the multistage bubble column, Δp_G with distances between the perforated plates greater than 400 mm can be equated with the hydrostatic pressure with sufficient accuracy within the investigated range,

$$\Delta p_G = \epsilon_L \frac{V}{F} \rho_L \cdot g, \qquad [16]$$

when V is the reactor volume and F is the cross sectional area of the column. For the smallest values φ of the perforated plates and the largest gas throughput, the hydrostatic pressure amounts to 80% of the total pressure drop. For the largest values of φ, it increased up to 95% total pressure drop. For calculating the pressure drop of the perforated plates the equations summarized by Mühle (1972) could be confirmed by these experiments.

Acknowledgement—Our experiments were made possible by the generous support of the firm Schering A. G., Bergkamen.

REFERENCES

BLASS, E. & KOCH, K. H. 1972 Strömungstechnische Untersuchungen an einem Blasensäulen-Kaskaden-Reaktor bei Gleichstrom von Gas und Flüssigkeit. *Chemie-Ing-Tech.* **44**, 913–921.

BLASS, E. & CORNELIUS, W. 1973 Betriebsverhalten von Blasensäulen-Kaskadenreaktoren. *Chemie-Ing-Tech.* **45**, 236–241.

CORNELIUS, W. 1975 Untersuchung der Verweilzeitverteilung von Flüssigkeit und Feststoff an zwei- und dreiphasigen Systemen in einem Blasensäulen-Kaskadenreaktor, Dissertation Techn. Universität Clausthal.

HADDAD, A. H. & WOLF, D. 1967 Residence time distribution function for multi-stage systems with backmixing. *Can. J. Chem. Engng* **45**, 100–104.

IMAFUKU, K., WANG, T. Y., KOIDE, D. & KUBOTA, H. 1968 The behaviour of suspended solid particles in the bubble column. *J. Chem-Engng. Jap.* **1**, 153–158.

KARDOS, J. 1969 Darstellung und Auswertung von Verweilzeitverteilungen nach dem Zellenmodell. *Chem. Tech.* **21**, 220 & 275–280.

KATS, M. B. & GENIN, L. 1966 Study of longitudinal mixing of liquid in cocurrent sparged reactors sectionalized with sieve trays. *Int. Chem. Engng* **7**, 246–253.

MACH, W. 1968 Impulsübergang im Dreiphasen-Fließbett, *Chemie-Ingr-Tech.* **40**, 1045–1050.

MOLZAHN, M. 1971 Die Verteilung des Feststoffs in einem dreiphasigen Blasensäulen-Reaktor ohne Flüssigkeitsumlauf, Dissertation Techn. Universität Berlin.

MÜHLE, J. 1972 Berechnung des trockenen Druckverlustes von Lochböden. *Chemie-Ing-Tech.* **44**, 72–79.

RICHARDS, W. & SPÖRRI, H. 1972 Verweilzeitverteilung in Bodenkolonnen. *Chemie-Ing-Tech.* **44**, 582–587.

SCHULZE-PILLOT, G. 1970 Verfahrenstechnische Untersuchungen mit radioaktiven Indikatoren. *Verfahrenstechnik* **6**, 208–212.